ACS OMEGA

Open Access

http://pubs.acs.org/journal/acsodf

Article

Investigation on the Gas Emission Law of Water-Containing Coal across the Rank Range

Zhen Wang, Guangli Huang, Xianfeng Liu,* Peng Liu,* Fujin Lin, Baisheng Nie, and Binyu Luo

Cite This: *ACS Omega* 2024, 9, 17289−17296

Read Online

ACCESS | Metrics & More | Article Recommendations

ABSTRACT: Water commonly occurs in coal reservoirs, and it can block the gas flow channels. This has a significant influence on methane transportation within coal. To reveal the gas emission law of water-containing coal across the rank range, three typical coal samples with different coal ranks covering lignite to anthracite were selected in this work. The initial velocity of gas emission (ΔP) under the effect of moisture was measured, and the combination of scanning electron microscopy and mercury injection method was adopted to study the pores and fracture characteristics within coal. Distribution features of oxygen-containing groups in coal were explored by X-ray photoelectron spectroscopy. The microscopic influence mechanism of the water content on ΔP in coal was also comprehensively elucidated. The experimental results show that the moisture content has an obvious inhibitory effect on the ΔP of coal, but the degree of influence on different coal rank samples was different. As the pore space of anthracite (sample XJ) is developed with numerous gas transportation channels, the ΔP has less changes at the lower moisture content (<4.36%). When the moisture content is >4.36%, a large number of water molecules will band together to form water clusters, hindering the gas release, thus greatly reducing the ΔP. However, the change of lignite (sample SL) shows an inverse trend to that of anthracite. Its ΔP is sensitive to the moisture content due to the small number of pores and low porosity. In addition, a great number of oxygen-containing groups in lignite can also provide good surface hydrophilicity for water molecules, and even a small amount of the moisture content (<3.21%) can block most of the pore and facture channels within coal, leading to the remarkable decrease in ΔP. For bituminous coal (sample ML), the distribution of pores and oxygen-containing groups is the most uniform, and the ΔP decreases linearly with the increase in the moisture content.

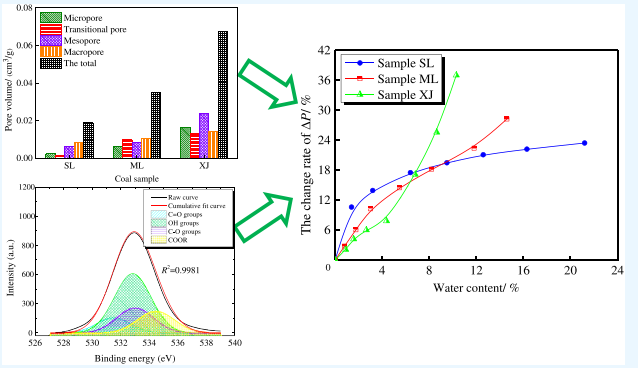

1. INTRODUCTION

With the depletion of shallow resources, coal mining is gradually marching to deep areas.[1−6] The occurrence conditions of deep coal seams are complicated, such as high ground stress, high gas, high heterogeneity, low permeability, low strength, and multiple structures, which undoubtedly increase the difficulty of gas control in coal mines in China.[7−15] As an effective means to prevent and control coal and gas outbursts, hydraulic antireflection technology (hydraulic fracturing, hydraulic punching, and hydraulic cutting) has been gradually promoted in China since the 1960s and has achieved good control effects.[16−20]

The initial velocity of coal gas emission (ΔP) reflects the ability of the coal body to release gas, which is widely used in coal mine production practice as an important coal and gas outburst prediction index.[21−25] It is generally believed that the greater the ΔP, the stronger the initial gas release capacity of the coal body, and the greater the risk of outburst.[26−29] After coal seam water injection, the surface of the coal body will be wetted and the ΔP will also change, which has been studied by many scholars. Crosdale et al.[30] found that there is a logarithmic function relationship between the ΔP and moisture content, and when the moisture content is 1.4−7.9%, ΔP is decreased the most with the increase in the moisture content. Wang et al.[31] established the relationship between the moisture content and ΔP and found that the two showed a linear negative correlation. Hao et al.[32] concluded that moisture occupies some of the pore fissures in coal, resulting in a decrease in the initial diffusion coefficient and initial desorption rate of gas with the increasing moisture content. Zhang et al.[33] found that the presence of water can reduce the amount of adsorbed gas in the coal, thus affecting the ΔP. Brennan et al.[34] experimentally proved that ΔP and the

Received: December 23, 2023
Revised: March 17, 2024
Accepted: March 20, 2024
Published: April 8, 2024

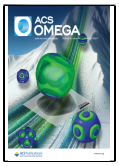

Table 1. Basic Industrial Parameters of the Coal Samples

sample no.	colliery	R_0 (%)	moisture (%)	ash (%)	volatile (%)	fix carbon (%)	coal type
SL	Shengli	0.41	12.61	7.52	46.22	33.65	lignite
ML	Malan	1.52	3.05	32.69	19.03	45.23	bituminous coal
XJ	Xinjing	2.39	2.72	15.41	8.54	73.33	anthracite

coefficient of coal solidity are greatly affected by the change of the moisture content and proposed that it is necessary to limit the moisture content of coal during the test of the outburst parameters. Svabova et al.[35] analyzed the law of the influence of the moisture content on the gas adsorption and emission characteristics of coal samples with different particle sizes and found that the smaller the particle size of coal samples, the greater the influence of moisture on the ΔP. Zhang et al.[36] showed that the ΔP was significantly reduced after water injection into the coal seam. When the moisture content of the coal seam is 7−10%, the outburst prevention effect is the best.

As mentioned above, a lot of research work has been carried out and more results have been achieved on the effect of the moisture content on coal gas desorption and emission characteristics.[37−40] Most of the experiments were conducted on coals with the same degree of metamorphism, and no systematic research has been carried out on coals across the rank range.[41−43] Based on the existing results, this paper carries out a study on the influence of different moisture contents on the initial velocity of gas emission in the coal body for three different metamorphic degree coal samples (lignite, bituminous coal, and anthracite) to reveal the mechanism of the influence of moisture in depth. The results of the study are of great significance for the prevention and control of gas hazards, outburst prediction, and risk assessments.[44−46]

2. MATERIALS AND METHODS

2.1. Coal Sample Preparation. Based on fully considering the type of coal rock and coal-forming period, the three kinds of coal samples used in the experiment were taken from the Shengli coal field in Inner Mongolia, Malan mine, and Xinjing mine in the Shanxi province. The fresh lump coal samples were collected from the working face with reference to the national standard GB/T482-2008, which were sealed, stored, and then sent to the laboratory immediately. The lump coal samples were crushed, ground, and screened, and the coal powder with a mass of about 10 g and a particle size of 60−80 mesh (0.20−0.25 mm) was selected for the determination of the vitrinite reflectance (R_0) and industrial analysis according to the national standards GB/T 6948-2008 and GB/T212-2008, respectively, and the basic industrial parameters of the coal samples obtained are shown in Table 1. From Table 1, it can be seen that the vitrinite reflectance of the three kinds of coal samples varied in the range of 0.41−2.39%, and samples SL, ML, and XJ belong to low-metamorphic lignite, medium-metamorphic bituminous coal, and high-metamorphic anthracite coal, respectively, which covered the three kinds of coal types with different metamorphic degrees.

Coal samples with different moisture contents were prepared by the method of wetting and then dried. First, the coal samples were put into hermetic bottles with pure water and moistened for 24 h to make the water fully wet the coal samples, dried naturally indoors, and then put into the vacuum drying box after the liquid water in the coal powder evaporated and then the moisture content of the coal was controlled by the control of drying time.

2.2. Experimental Methods. The method of variable capacity and pressure was adopted in the test of the initial velocity of gas emission (ΔP) for the coal samples with different moisture contents. After checking the air tightness, 3.5 g of coal samples with a particle size of 60−80 was weighed and put into the specimen bottle, and after 1.5 h of vacuum degassing, the inflation valve was opened, methane was filled into the specimen bottle, the inflation pressure was kept at 0.1 mpa, and the measurement of ΔP was started after the adsorption of gas for 1.5 h. The instrument used for the experiment was the WT-1 type fully automatic initial velocity of the gas emission tester, and the measurement error was <1 mmHg. The test process was referred to AQ1080-2009.

The pores and cracks in coal are the channels for gas transportation, and different pore and crack structures directly affect the initial velocity of gas emission from the coal body. Using scanning electron microscopy (SEM) was adopted to directly observe the pore and fissure morphology of the coal samples; the pore structure parameters of the coal body were obtained by the mercuric pressure method, the instrument used was a 02111- 1PoreMaster-60 automatic mercuric pressure, and the testing process was carried out in accordance with GB/T 21650.1-2008. The structural parameters such as the pore diameter and pore volume of the coal samples were solved by the calculation software of the instrument. Given the fact that water molecules are prone to bond with polar chemical groups (e.g., hydroxyl groups and carboxyl groups) within coal, X-ray photoelectron spectroscopy (XPS) was adopted to detect the oxygen-containing groups using a surface analysis instrument (ESCALAB250 Xi) in an ultrahigh vacuum system under room temperature. After the survey spectra were scanned, the high-resolution spectra were collected for the pulverized coal samples at a step of 0.05 eV under a pass energy of 20 eV. Prior to data processing, the binding energy should be corrected via assigning the C 1s hydrocarbon peak around 284.6 eV. Peak fitting was carried out after background subtraction using the XPS software.

3. RESULTS AND DISCUSSION

3.1. Gas Emission Characteristics of Water-Containing Coal Samples. The variation curves of the initial velocity of gas emission (ΔP) of coal samples with different moisture contents are shown in Figure 1. As the figure shows, moisture has an obvious inhibiting effect on the initial velocity of gas emission of all three coal samples: ΔP of samples SL and XJ decreased from 8.09 and 33.17 mmHg to 6.18 and 21.06 mmHg, with decreasing amplitudes of 23.61 and 36.51%, respectively; the ΔP of sample ML decreased from 21.42 to 15.36 mmHg with a decreasing amplitude of 28.29%. Comparing the ΔP change curves of the three kinds of coal samples under the influence of different moisture contents, it can be found that the ΔP of sample XJ has the largest decrease, and sample SL has the smallest decrease. Sample XJ belongs to the high-metamorphic anthracite, and sample SL belongs to the lignite with the lowest metamorphic degree, which indicates that the higher the coal rank, the larger the influence of the moisture content on the initial velocity of gas emission.

https://doi.org/10.1021/acsomega.3c10295
ACS Omega 2024, 9, 17289−17296

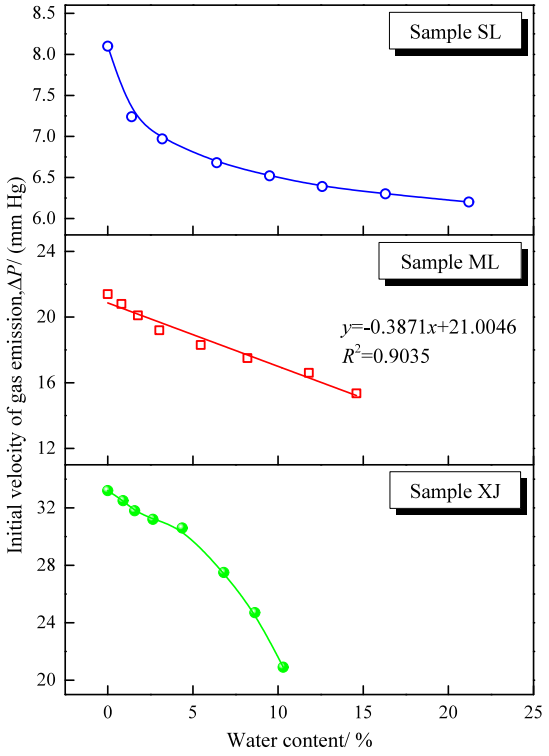

Figure 1. Variation curve of the initial velocity of gas emission in coal samples with different moisture contents.

Figure 2 shows the rate of change of the initial velocity of gas emission with the moisture content. From the figure, it can be seen that the ΔP change rate varies at different moisture content intervals. For sample SL, when the moisture content is in the range of 0−3.21%, the ΔP change rate is larger, and the initial velocity of gas emission decreases rapidly with the increase in the moisture content; when the moisture content is more than 3.21%, the ΔP change rate increases slightly and tends to be stable, and the initial velocity of gas emission decreases slowly and stabilizes gradually. For sample ML, the rate of change of ΔP increases steadily with the increase in the moisture content, and the initial velocity of gas emission shows a good linear negative correlation with the moisture content. For sample XJ, when the moisture content is less than 4.36%, the ΔP change rate is small, and the initial velocity of gas emission decreases slowly with the increase in the moisture content (Figure 1), and when the moisture content is more than 4.36%, the ΔP change rate increases sharply, and the initial velocity of gas emission decreases rapidly.

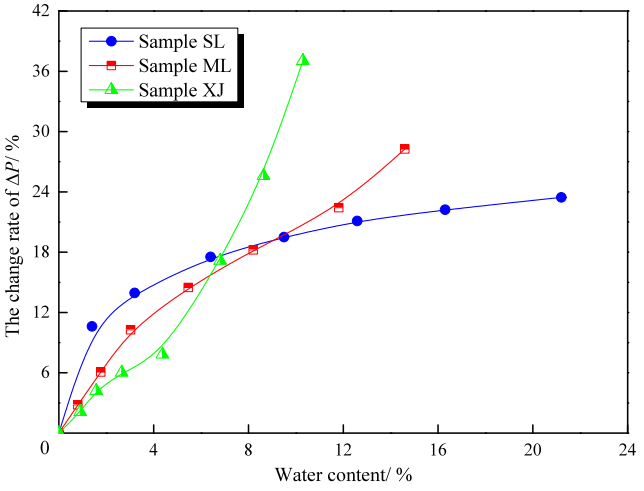

Figure 2. Change rate of initial velocity of gas emission with the moisture content.

3.2. Pore Structure of Coal Samples. The results of scanning electron microscopy of each coal sample are shown in Figure 3. As can be seen from the figure, the surface morphology of these three kinds of coal samples differed significantly. The surface of sample SL is relatively flat, containing some wedge-shaped pores, and the pore diameter is large, mostly on the order of micrometers. The surface of sample ML is rougher, containing more elliptical pores and ink-bottle pores. However, the surface of sample XJ is the roughest, the slit-shape pores are widely distributed, the pore diameter is smaller, and the pores are the most developed.

To quantitatively study the pore distribution characteristics of each coal sample, this paper adopts the Hodot pore classification standard, i.e., micropores (<10 nm), transitional pores (10−100 nm), mesopores (100−1000 nm), and macropores (>1000 nm).[47,48] The mercury intrusion curves of the studied coal samples are presented in Figure 4. The cumulative mercury volume of sample XJ is the largest. Figure 5 shows the results of the pore distribution of each coal sample obtained by the mercury pressure method. It can be seen that sample SL has a higher proportion of mesopores and macropores, sample ML has a more uniform pore distribution with a small difference in the volume of each type of pore, and sample XJ is dominated by micropores and mesopores. In each type of pores, the order of pore volume is XJ > ML > SL, which indicates that the pore distribution and development degree of coal samples with different metamorphic degrees differ significantly. The pore volume of anthracite is highly developed and abundant in all types of pores followed by bituminous coal, and lignite has the least pore volume.

3.3. Distribution of Oxygen-Containing Groups within Coal. To identify the surface chemical groups of coal, a wide XPS spectrum was acquired with a binding energy of 0−1400 eV. Figure 6 shows the typical XPS spectrum of the studied coal samples. The oxygen and carbon peaks are distinctly identified, illustrating the major components of the coal surface. A weak nitrogen peak (N 1s) is also recognized at a binding energy of around 400 eV, implying the existence of a few nitrogen-containing groups. Compared with the O 1s peak, the N 1s peak is almost ignored. Thus, the impact of oxygen-containing groups on surface hydrophilicity and gas flow is highlighted in this study. It is apparent that sample SL has the largest O 1s peak, while sample XJ has the least. The C 1s peak demonstrates the opposite changing trend, indicating that sample XJ contains developed aromatic carbons. The typical curve-fitting of the XPS spectrum was performed at the O 1s peak region with binding energy ranging from 527 to 539 eV. As shown in Figure 7, good fits ($R^2 > 0.99$) between the raw curves and cumulative fit curves are obtained using Gaussian/Lorentzian peak shapes. It can be seen that all the O 1s peaks can be decomposed into four small peaks at binding energies of 531.3, 532.2, 533.0, and 534.3 eV. These four peaks are attributed to C═O groups, OH groups, C−O groups, and COOR groups, respectively.[49−51] For quantitative analysis, the peak area is used as an index to reflect the content of functional groups in coal.[52−55] Distribution of oxygen-containing groups within coal samples is presented in Figure 8. Obviously, OH groups account for the greatest

https://doi.org/10.1021/acsomega.3c10295
ACS Omega 2024, 9, 17289−17296

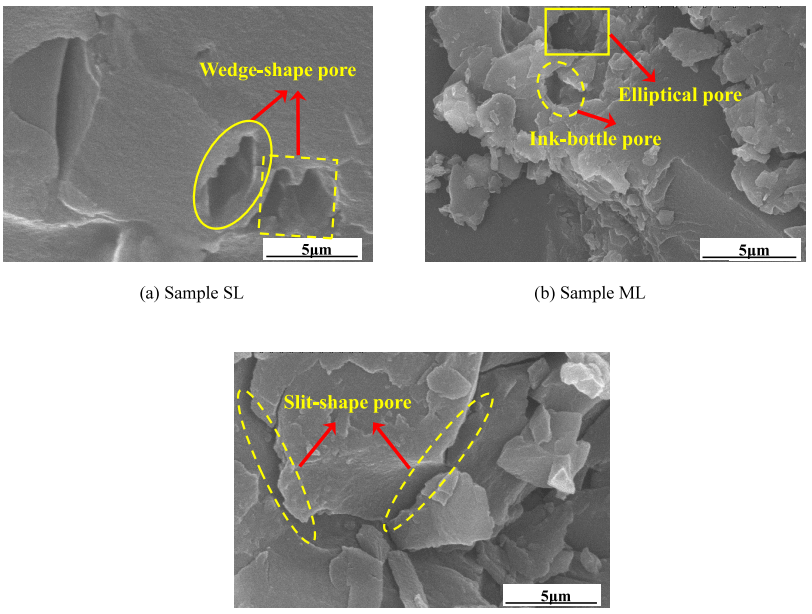

(a) Sample SL (b) Sample ML

(c) Sample XJ

Figure 3. (a−c) Scanning electron microscopy diagrams of coal samples.

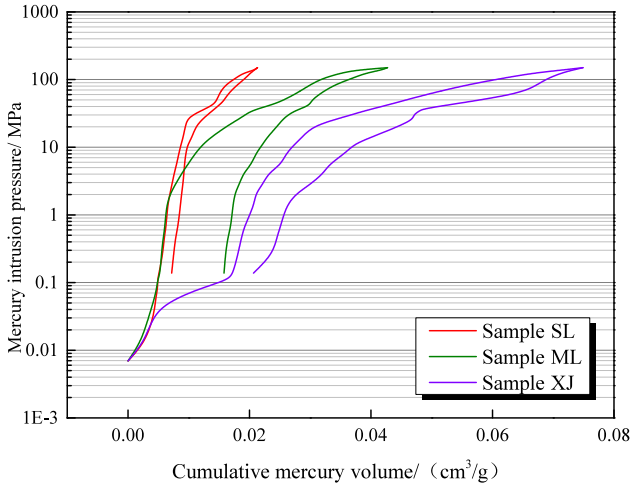

Figure 4. Mercury intrusion curves of the studied coal samples

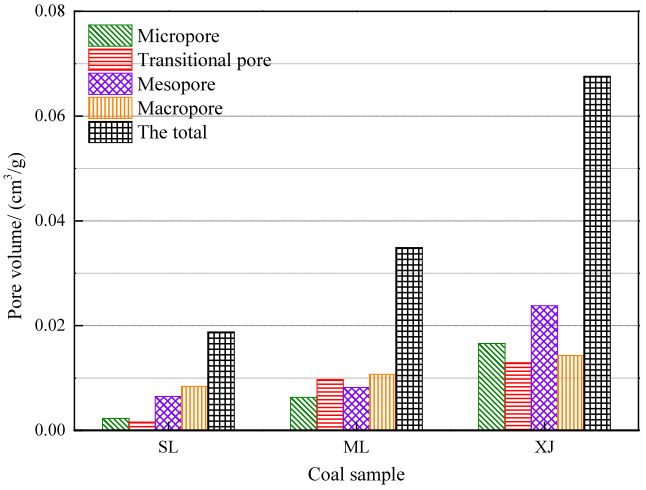

Figure 5. Pore size distribution of coal samples.

proportions (36.83−56.25%) among all the oxygen-containing groups followed by C−O groups. Sample SL has the highest content of total oxygen-containing groups, which is 0.68 and 3.81 times larger than samples ML and XJ, respectively. Thus, the oxygen-containing groups are more complicated in low-rank coals, especially for lignite. These oxygen-containing groups usually serve as side chains or cross-linking bonds in the surface molecular structures of the coal samples.

3.4. Influence of Moisture on the Initial Velocity of Gas Emission. Since the presence of moisture will occupy the coal surface space, some of the pore cracks are blocked by water molecules, resulting in the reduction of gas transportation channels. As a result, the initial velocity of gas emission of the above coal samples decreased significantly under the effect of moisture, but the degree of influence on different coal rank samples was different. With the increase in the moisture content, the initial velocity of gas emission of sample SL decreased rapidly and then decreased slowly, ΔP of sample ML decreased linearly, and ΔP of sample XJ decreased slightly and then decreased rapidly after exceeding a certain moisture content. The differences in the effect of moisture on the initial velocity of gas velocity of lignite, bituminous coal, and anthracite are related to the distribution of pores in the coal body.

Influencing the mechanism of the moisture content on methane emission within coal is illustrated in Figure 9. Both surface chemical groups and pore/fracture distribution play a vital role in gas emission of water-containing coal. Combined with the pore structure test results, the total pore volumes of anthracite (sample XJ), bituminous coal (sample ML), and lignite (sample SL) are 0.0676, 0.0349, and 0.0188 cm^3/g, respectively, and the former is 1.94 and 3.6 times more than the latter two. As the pore space of anthracite (sample XJ) is developed with numerous gas transportation channels, the number of oxygen-containing groups is also quite limited (Figure 8). When the moisture content is low (<4.36%), competitive adsorption between methane and water molecules will occur in oxygen-containing groups.[56−60] Though part of the pore space is occupied by water molecules, there are still enough

https://doi.org/10.1021/acsomega.3c10295
ACS Omega 2024, 9, 17289−17296

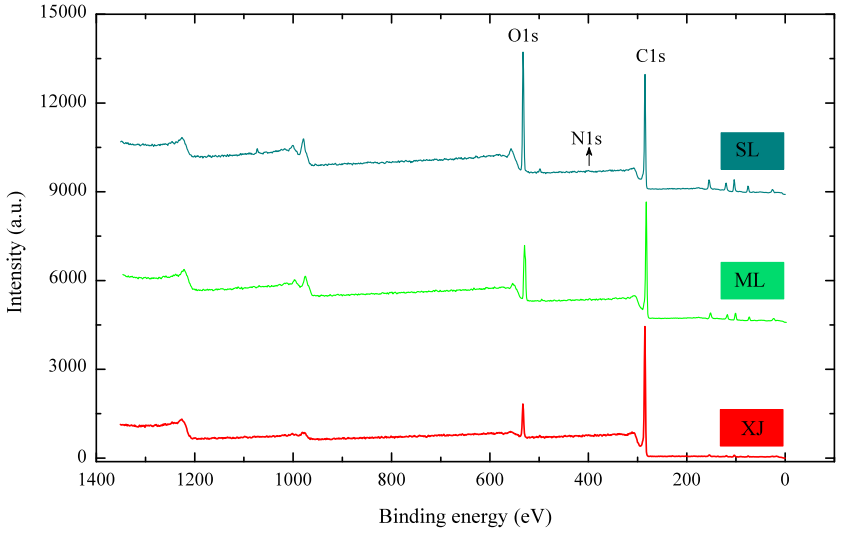

Figure 6. XPS spectrum of the studied coal samples.

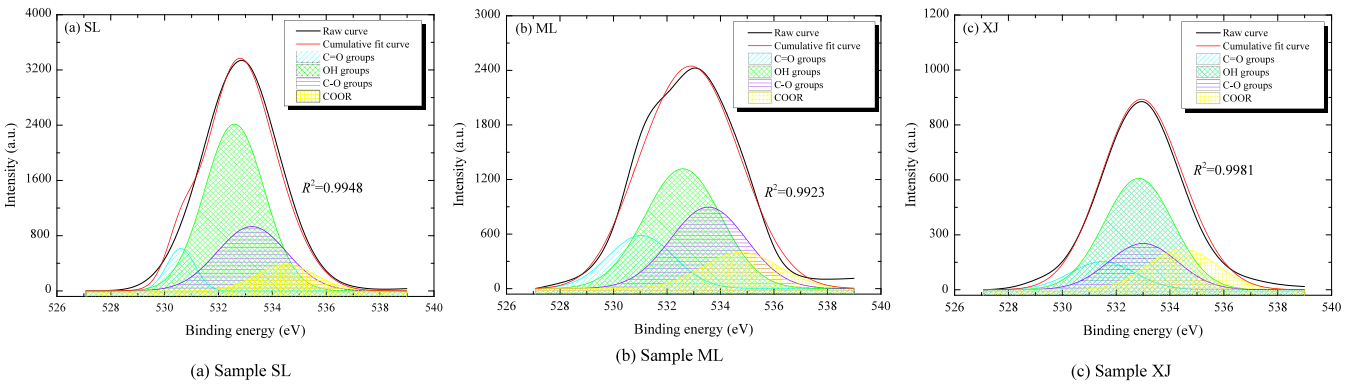

Figure 7. (a−c) Curve-fitting analysis of the XPS spectrum.

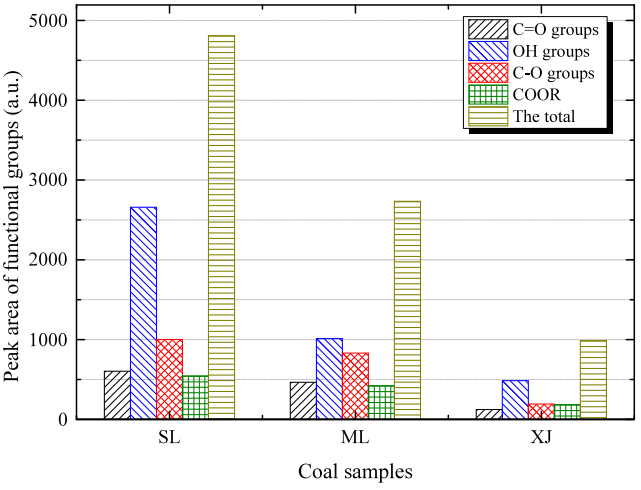

Figure 8. Distribution of oxygen-containing groups within the coal samples.

gas diffusion channels; therefore, the moisture content does not have much effect on the initial velocity of gas emission. Once the moisture content exceeds 4.36%, a large number of water molecules will band together to form water clusters (Figure 9). These large clusters will occupy more pore cracks, hindering gas release and thus greatly reducing the initial velocity of gas discharge. For lignite (sample SL), due to the small number of pores and low porosity, the number of channels for gas transportation is limited. On the other hand, a great number of oxygen-containing groups are found in lignite (Figure 8), which can provide good surface hydrophilicity. Water molecules are prone to bond with these polar groups; thus, even a small amount of the moisture content can block most of the pore and fracture channels within coal. It is not strange that when the moisture content is low (<3.21%), the inhibitory effect of moisture is also very significant. With the increase in the moisture content (>3.21%), the effect of moisture will gradually weaken, and the initial velocity of gas emission will slowly decrease until it becomes stabilized. For bituminous coal (sample ML), the distribution of pores and oxygen-containing groups is the most uniform, the connectivity of pores is good, and the initial velocity of gas emission decreases linearly with the increase in the moisture content. In addition, coals have numerous adsorption sites for water molecules and consequently they have significant swelling potential upon water adsorption. The higher adsorption capacity and the swelling potential can lead to a significant alteration in the coal porosity.[61−63] This also leads to the decrease in migration channels and affects gas emissions within coal, which will be further studied in our future work.

https://doi.org/10.1021/acsomega.3c10295
ACS Omega 2024, 9, 17289−17296

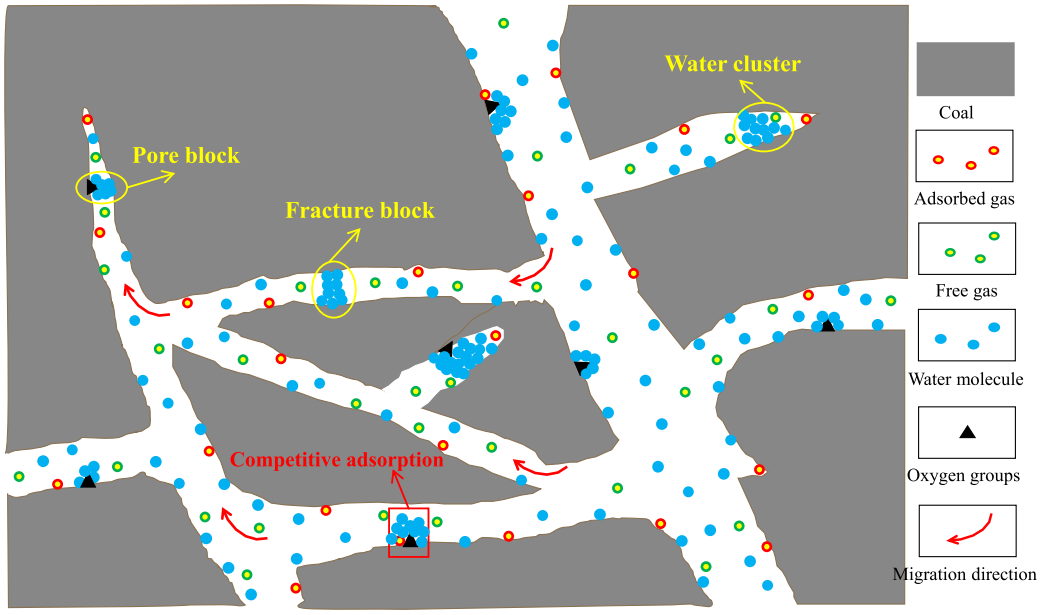

Figure 9. Influencing mechanism of the moisture content on methane emission within coal.

4. CONCLUSIONS

In this paper, taking coal samples with different degrees of metamorphism as the research object, we studied the influence law of different moisture contents on the characteristics of the coal gas emission, and combined with the pore distribution characteristics of the coal body, we elucidated the mechanism of the influence of moisture on the initial velocity of gas emission of coal samples. The following main conclusions were obtained:

1. Under the effect of moisture, the initial velocity of gas emission of coal samples decreased significantly, and the maximum decreases in the initial velocity of gas emission of samples SL, ML, and XJ were 23.61, 28.29, and 36.51%, respectively, which indicated that the higher the coal rank, the greater the effect of the moisture content on the initial velocity of gas emission.
2. The pore structure of each sample varied significantly: high proportion of mesopores and macropores in sample SL; more uniform distribution of pores in sample ML and similar pore volume in each type; micropores and mesopores dominated in the XJ sample. In each type of pore, the order of pore volume is sample XJ > sample ML > sample SL.
3. The differences in the effects of moisture on the initial velocity of gas emission of lignite, bituminous coal, and anthracite are related to the pore distribution of the coal body. With the increase in the moisture content, the initial velocity of gas emission of lignite decreased rapidly and then decreased slowly, ΔP of bituminous coal decreased linearly, and the initial velocity of gas emission of anthracite decreased slightly and then decreased sharply.

AUTHOR INFORMATION

Corresponding Authors

Xianfeng Liu − *State Key Laboratory of Coal Mine Disaster Dynamics and Control, School of Resources and Safety Engineering, Chongqing University, Chongqing 400044, China; State Key Laboratory for Fine Exploration and Intelligent Development of Coal Resources, China University of Mining and Technology, Xuzhou, Jiangsu 221116, China;* orcid.org/0000-0002-0368-014X; Phone: +86 02365105093; Email: cumtblxf@163.com

Peng Liu − *State Key Laboratory of Coal Mine Disaster Dynamics and Control, School of Resources and Safety Engineering, Chongqing University, Chongqing 400044, China*; Email: rocliu@cqu.edu.cn

Authors

Zhen Wang − *State Key Laboratory of the Gas Disaster Detecting, Preventing and Emergency Controlling, China Coal Technology and Engineering Group Chongqing Research Institute, Chongqing 400037, China; State Key Laboratory of Coal Mine Disaster Dynamics and Control, School of Resources and Safety Engineering, Chongqing University, Chongqing 400044, China*

Guangli Huang − *State Key Laboratory of the Gas Disaster Detecting, Preventing and Emergency Controlling, China Coal Technology and Engineering Group Chongqing Research Institute, Chongqing 400037, China; State Key Laboratory of Coal Mine Disaster Dynamics and Control, School of Resources and Safety Engineering, Chongqing University, Chongqing 400044, China*

Fujin Lin − *State Key Laboratory of the Gas Disaster Detecting, Preventing and Emergency Controlling, China Coal Technology and Engineering Group Chongqing Research Institute, Chongqing 400037, China; State Key Laboratory of Coal Mine Disaster Dynamics and Control, School of Resources and Safety Engineering, Chongqing University, Chongqing 400044, China*

Baisheng Nie − *State Key Laboratory of Coal Mine Disaster Dynamics and Control, School of Resources and Safety Engineering, Chongqing University, Chongqing 400044, China*

Binyu Luo − *Hubei Key Laboratory for Efficient Utilization and Agglomeration of Metallurgic Mineral Resources, Wuhan University of Science and Technology, Wuhan 430081, China*

Complete contact information is available at: https://pubs.acs.org/10.1021/acsomega.3c10295

https://doi.org/10.1021/acsomega.3c10295
ACS Omega 2024, 9, 17289−17296

Notes

The authors declare no competing financial interest.
No potential conflict of interest was reported by the authors.

■ ACKNOWLEDGMENTS

This work was financially supported by the National Natural Science Foundation of China (grant no. 52274173), the Open Research Fund of State Key Laboratory of the Gas Disaster Detecting, Preventing and Emergency Controlling, China Coal Technology and Engineering Group Chongqing Research Institute (nos. 2021SKLFF03 and 2022SKLKF04), the Open Research Fund of the Hubei Key Laboratory for Efficient Utilization and Agglomeration of Metallurgic Mineral Resources, Wuhan University of Science and Technology (2022zy001), and the Open Research Fund of the State Key Laboratory for Fine Exploration and Intelligent Development of Coal Resources, CUMT (SKLCRSM22KF005).

■ REFERENCES

(1) Mwakipunda, G. C.; Wang, Y.; Mgimba, M. M.; et al. Recent Advances in Carbon Dioxide Sequestration in Deep Unmineable Coal Seams Using CO_2-ECBM Technology: Experimental Studies, Simulation, and Field Applications. *Energy Fuels* **2023**, *37*, 17161−17186.
(2) Wang, W.; Lu, X.; Chen, X.; et al. Spatiotemporal Relationship for Well-Type Selection and Layout Optimization of Surface Wells Based on the REV Permeability Model. *ACS Omega* **2023**, *8*, 46127−46143.
(3) Zou, Y.; Liu, X.; Nie, B.; et al. Quantitative Evaluation of the Influence of Injected Water on Methane Desorption Behaviors of Coal in the Ordos Basin. *Energy Fuels* **2023**, *37*, 17227−17237.
(4) Liu, X.; Zhang, C.; Nie, B.; Zhang, C.; Song, D.; Yang, T.; Ma, Z. Mechanical response and mineral dissolution of anthracite induced by supercritical CO_2 saturation: Influence of saturation time. *Fuel* **2022**, *319*, No. 123759.
(5) Malinnikova, O. N.; Ul'yanova, E. V.; Kharchenko, A. V.; et al. Influence of coal microstructure on gas content of the face area. *Journal of Mining Science* **2020**, *56*, 351−358.
(6) Liao, Z.; Liu, X.; Song, D.; He, X.; Nie, B.; Yang, T.; Wang, L. Micro-structural damage to coal induced by liquid CO_2 phase change fracturing. *Natural Resources Research* **2021**, *30* (2), 1613−1627.
(7) Lanetc, Z.; Zhuravljov, A.; Jing, Y.; et al. Coupling of transient matrix diffusion and pore network models for gas flow in coal. *Journal of Natural Gas Science and Engineering* **2021**, *88*, No. 103741.
(8) Liu, X.; Jia, X.; Niu, Y.; Nie, B.; Zhang, C.; Song, D. Alterations in coal mechanical properties and permeability influenced by liquid CO_2 phase change fracturing. *Fuel* **2023**, *354*, No. 129254.
(9) Zhang, B.; Wang, H.; Wang, P.; et al. Experimental and theoretical study on the dynamic effective stress of loaded gassy coal during gas release. *International Journal of Mining Science and Technology* **2023**, *33* (3), 339−349.
(10) Liu, X.; Nie, B.; Wang, W.; Wang, Z.; Zhang, L. The use of AFM in quantitative analysis of pore characteristics in coal and coalbearing shale. *Marine and Petroleum Geology* **2019**, *105*, 331−337.
(11) Kong, X.; He, D.; Liu, X.; Wang, E.; Li, S.; Liu, T.; Ji, P.; Deng, D.; Yang, S. Strain characteristics and energy dissipation laws of gas-bearing coal during impact fracture process. *Energy* **2022**, *242*, No. 123028.
(12) Khani, A.; Baghbanan, A.; Hashemolhosseini, H. Numerical investigation of the effect of fracture intensity on deformability and REV of fractured rock masses. *Int. J. Rock Mech Min Sci.* **2013**, *63*, 104−112.
(13) Chen, K.; Liu, X.; Wang, L.; Song, D.; Nie, B.; Yang, T. Influence of sequestered supercritical CO_2 treatment on the pore size distribution of coal across the rank range. *Fuel* **2021**, *306*, No. 121708.
(14) Liu, X.; Jia, X.; Liu, W.; Nie, B.; Zhang, C.; Song, D. Mechanical strength and porosity changes of bituminous coal induced by supercritical CO_2 interactions: Influence of saturation pressure. *Geoenergy Science and Engineering* **2023**, *225*, No. 211691.
(15) Masoudian, M. S. Multiphysics of carbon dioxide sequestration in coalbeds: A review with a focus on geomechanical characteristics of coal. *Journal of Rock Mechanics and Geotechnical Engineering* **2016**, *8* (1), 93−112.
(16) Ebadi, M.; Orlov, D.; Makhotin, I.; et al. Strengthening the digital rock physics, using downsampling for sub-resolved pores in tight sandstones. *Journal of Natural Gas Science and Engineering* **2021**, *89*, No. 103869.
(17) Karayiğit, A.İ.; Mastalerz, M.; Oskay, R. G.; et al. Meso-and microporosity of the subbituminous kM2 coal seam (Soma, Turkey) and its relationship with coal characteristics. *Int. J. Coal Geol.* **2017**, *184*, 73−87.
(18) Swanson, S. M.; Mastalerz, M. D.; Engle, M. A.; et al. Pore characteristics ofWilcox group coal, US Gulf Coast region: implications for the occurrence of coalbed gas. *Int. J. Coal Geol.* **2015**, *139*, 80−94.
(19) Sun, B.; Zhu, J.; Chen, Z.; et al. Multiscale pore distribution and evolution characteristic of medium/low-rank coal. *Arabian J. Geosci.* **2022**, *15* (23), 1743.
(20) Liu, X.; Nie, B.; Guo, K.; Zhang, C.; Wang, Z.; Wang, L. Permeability enhancement and porosity change of coal by liquid carbon dioxide phase change fracturing. *Engineering Geology* **2021**, *287*, No. 106106.
(21) Hattingh, B. B.; Everson, R. C.; Neomagus, H. W. J. P.; Bunt, J. R.; van Niekerk, D.; Jordaan, J. H. L.; et al. Elucidation of the structural and molecular properties of typical South African coals. *Energy Fuel* **2013**, *27* (6), 3161−3172.
(22) Howaniec, N. Development of porous structure of lignite chars at high pressure and temperature. *Fuel Process. Technol.* **2016**, *154*, 163−167.
(23) Drelich, J.; Laskowski, J. S.; Pawlik, M.; et al. Preparation of a coal surface for contact angle measurements. *J. Adhes. Sci. Technol.* **1997**, *11* (11), 1399−1431.
(24) Carbone, F.; Beretta, F.; D'Anna, A. A flat premixed flame reactor to study nano-ash formation during high temperature pulverized coal combustion and oxygen firing. *Fuel* **2011**, *90* (1), 369−375.
(25) Cui, B.; Feng, G.; Bai, J.; et al. Failure characteristics and the damage evolution of a composite bearing structure in pillar-side cemented paste backfilling. *International Journal of Minerals, Metallurgy and Materials* **2023**, *30*, 1524−1537.
(26) Soleimani, F.; Si, G.; Roshan, H.; Zhang, Z. Numerical modelling of coal and gas outburst initiation using energy balance principles. *Fuel* **2023**, *334*, No. 126687.
(27) Liu, X.; Song, D.; He, X.; et al. Quantitative analysis of coal nanopore characteristics using atomic force microscopy. *Powder Technol.* **2019**, *346*, 332−340.
(28) Liu, H.; Wang, L.; Xie, G. X. Dynamic Compression Behavior of Coal Under Different Initial Gas Pressures. *Rock Mechanics and Rock Engineering* **2023**, *56* (3), 2213−2228.
(29) Labani, M. M.; Rezaee, R.; Saeedi, A.; et al. Evaluation of pore size spectrum of gas shale reservoirs using low pressure nitrogen adsorption, gas expansion and mercury porosimetry: a case study from the Perth and canning basins, Western Australia. *J. Pet. Sci. Eng.* **2013**, *112*, 7−16.
(30) Crosdale, P. J.; Moore, T. A.; Mares, T. E. Influence of moisture content and temperature on methane adsorption isotherm analysis for coals from a low-rank, biogenically-sourced gas reservoir. *International Journal of Coal Geology* **2008**, *76* (1), 166−174.
(31) Wang, K.; Zang, J.; Feng, Y.; Wu, Y. Effects of moisture on diffusion kinetics in Chinese coals during methane desorption. *Journal of Natural Gas Science and Engineering* **2014**, *21*, 1005−1014.
(32) Hao, M.; Wei, C.; Qiao, Z. Effect of internal moisture on CH4 adsorption and diffusion of coal: A molecular simulation study. *Chem. Phys. Lett.* **2021**, *783*, No. 139086.
(33) Zhang, Q.; Liu, X.; Nie, B.; Wu, W.; Wang, R. Methane sorption behavior on tectonic coal under the influence of moisture. *Fuel* **2022**, *327*, No. 125150.
(34) Brennan, J. K.; Thomson, K. T.; Gubbins, K. E. Adsorption of water in activated carbons: Effects of pore blocking and connectivity. *Langmuir* **2002**, *18* (14), 5438−5447.

https://doi.org/10.1021/acsomega.3c10295
ACS Omega 2024, 9, 17289−17296

(35) Svabova, M.; Weishauptova, Z.; Pribyl, O. Water vapour adsorption on coal. *Fuel* **2011**, *90* (5), 1892−1899.
(36) Zhang, K.; Cheng, Y.; Wang, L.; Dong, J.; Hao, C.; Jiang, J. Pore morphology characterization and its effect on methane desorption in water-containing coal: An exploratory study on the mechanism of gas migration in water-injected coal seam. *Journal of Natural Gas Science and Engineering* **2020**, *75*, No. 103152.
(37) Lanetc, Z.; Zhuravljov, A.; Armstrong, R. T.; et al. Hybrid numerical methods for modelling multi-physics mass transport in coal. *Int. J. Heat Mass Transfer* **2023**, *214*, 124386.
(38) Liu, X.; Nie, B. Fractal characteristics of coal samples utilizing image analysis and gas adsorption. *Fuel* **2016**, *182*, 314−322.
(39) Wang, L.; Ni, S.; Wang, H.; et al. Influence of wettability alteration on water-blocking effect and gas desorption of coal. *Process Safety and Environmental Protection* **2023**, *180*, 361−374.
(40) Zhao, J.; Tian, S.; Xie, H.; et al. Study of time-varying laws of stability and wettability of SiO_2−H_2O nanofluids with different particle sizes. *Ind. Eng. Chem. Res.* **2023**, *62* (34), 13529−13540.
(41) Keshavarz, A.; Sakurovs, R.; Grigore, M.; et al. Effect of maceral composition and coal rank on gas diffusion in Australian coals. *International Journal of Coal Geology* **2017**, *173*, 65−75.
(42) Ul'Yanova, E. V.; Malinnikova, O. N.; Burchak, A. V.; Balalaev, A. K.; Baranovsky, V. I. Gas content and structure of coal in donets basin. *Journal of Mining Science* **2018**, *53* (4), 655−662.
(43) Nie, B.; Liu, X.; Yang, L.; Meng, J.; Li, X. Pore structure characterization of different rank coals using gas adsorption and scanning electron microscopy. *Fuel* **2015**, *158*, 908−917.
(44) Baatar, L.; Mostaghimi, P.; Yuan, M.; Armstrong, R. T.; Adler, L.; Canbulat, I.; Si, G.; Gaidarov, B.; Jing, Y. Multiscale measurements of gas diffusion coefficient of coal using counter-diffusion and imagebased methods. *International Journal of Coal Geology* **2023**, *265*, No. 104155.
(45) Ma, Y.; Nie, B.; He, X.; et al. Mechanism investigation on coal and gas outburst: an overview. *International Journal of Minerals, Metallurgy and Materials* **2020**, *27*, 872−887.
(46) Pajdak, A. Studies on the influence of moisture on the sorption and structural properties of hard coals. *International Journal of Greenhouse Gas Control* **2020**, *103*, No. 103193.
(47) Tanis-Kanbur, M. B.; Peinador, R. I.; Calvo, J. I.; et al. Porosimetric membrane characterization techniques: A review. *J. Membr. Sci.* **2021**, *619*, No. 118750.
(48) Liu, X.; Kong, X.; Nie, B.; Song, D.; He, X.; Wang, L. Pore fractal dimensions of bituminous coal reservoirs in north china and their impact on gas adsorption capacity. *Natural Resources Research* **2021**, *30* (6), 4585−4596.
(49) Grzybek, T.; Pietrzak, R.; Wachowska, H. X-ray photoelectron spectroscopy study of oxidized coals with different sulphur content. *Fuel Process. Technol.* **2002**, *77*, 1−7.
(50) Pietrzak, R.; Grzybek, T.; Wachowska, H. XPS study of pyrite-free coals subjected to different oxidizing agents. *Fuel.* **2007**, *86*, 2616−2624.
(51) Chen, K.; Liu, X.; Nie, B.; Zhang, C.; Song, D.; Wang, L.; Yang, T. Mineral dissolution and pore alteration of coal induced by interactions with supercritical CO_2. *Energy* **2022**, *248*, No. 123627.
(52) He, X.; Liu, X.; Nie, B.; Song, D. FTIR and Raman spectroscopy characterization of functional groups in various rank coals. *Fuel* **2017**, *206*, 555−563.
(53) Iglesias, M. J.; Jiménez, A.; Laggoun-Défarge, F.; Suarez-Ruiz, I. FTIR study of pure vitrains and associated coals. *Energy Fuel* **1995**, *9*, 458−466.
(54) Fletcher, T. H.; Gillis, R.; Adams, J.; Hall, T.; Mayne, C. L.; Solum, M. S.; Pugmire, R. J. Characterization of macromolecular structure elements from a Green River oil shale, II. Characterization of pyrolysis products by 13C NMR, GC/MS, and FTIR. *Energy Fuel* **2014**, *28*, 2959−2970.
(55) Okolo, G. N.; Neomagus, H. W.; Everson, R. C.; Roberts, M. J.; Bunt, J. R.; Sakurovs, R.; Mathews, J. P. Chemical−structural properties of South African bituminous coals: insights from wide angle XRD−carbon fraction analysis, ATR−FTIR, solid state 13 C NMR, and HRTEM techniques. *Fuel* **2015**, *158*, 779−792.
(56) Liu, X.; Wang, L.; Kong, X.; Ma, Z.; Nie, B.; Song, D.; Yang, T. Role of pore irregularity in methane desorption capacity of coking coal. *Fuel* **2022**, *314*, No. 123037.
(57) O'Neill, K. T.; Birt, B.; Hopper, T. Borehole measurements of adsorbed gas content in coals using stimulated diffusion nuclear magnetic resonance. *International Journal of Coal Geology* **2021**, *247*, No. 103845.
(58) Wang, G.; Li, Y.; Wang, E.; Huang, Q.; Wang, S.; Li, H. Experimental study on preparation of nanoparticle-surfactant nanofluids and their effects on coal surface wettability. *Int. J. Min. Sci. Technol.* **2022**, *32* (2), 387−397.
(59) Solum, M. S.; Mayne, C. L.; Orendt, A. M.; Pugmire, R. J.; Adams, J.; Fletcher, T. H. Characterization of macromolecular structure elements from a Green River oil shale, I. Extracts. *Energy Fuel* **2014**, *28*, 453−465.
(60) Sharma, R. V.; Kumar, S.; Adak, A. K.; et al. A comparative study of molecular structure and combustion behavior of coal and its separated vitrains. *J. Mol. Struct.* **2024**, *1299*, No. 137152.
(61) Haque, M. F. Nonlinear anisotropic finite element analysis of liquefiable tunnel−sand−pile interaction under seismic excitation. *Deep Underground Science and Engineering* **2023**, *2* (3), 275−285.
(62) Lyu, J.; Qi, L.; Wang, X.; et al. Analysis of the impact of the combined use of rebar bolts and FRP bolts in the roadway enclosure. *Sci. Rep.* **2023**, *13* (1), 19630.
(63) Wang, J.; Xie, H.; Leung, C.; et al. New understandings on initiation and evolution of disasters in deep underground. *Deep Underground Science and Engineering* **2023**, *2* (3), 205−206.

https://doi.org/10.1021/acsomega.3c10295
ACS Omega 2024, 9, 17289−17296